

Lithium, Sodium, and Potassium Abundances in Sharp-Lined A-Type Stars *

Yoichi TAKEDA,¹ Dong-Il KANG,² Inwoo HAN,³ Byeong-Cheol LEE,³
Kang-Min KIM,³ Satoshi KAWANOMOTO,¹ and Naoko OHISHI¹
¹National Astronomical Observatory, 2-21-1 Osawa, Mitaka, Tokyo 181-8588
takeda.yoichi@nao.ac.jp, kawanomoto.satoshi@nao.ac.jp, naoko.ohishi@nao.ac.jp
²Gyeongsangnamdo Institute of Science Education,
75-18 Gajinri, Jinsungmyeon, Jinju, Gyeongnam 660-851, Korea
kangdongil@gmail.com

³Korea Astronomy and Space Science Institute, 61-1 Whaam-dong, Youseong-gu, Taejeon 305-348, Korea
iwhan@kasi.re.kr, bcllee@kasi.re.kr, kmkim@kasi.re.kr

(Received 2011 September 29; accepted 2011 October 22)

Abstract

The abundances of alkali elements (Li, Na, and K) were determined from the Li I 6708, Na I 5682/5688, and K I 7699 lines by taking into account the non-LTE effect for 24 sharp-lined A-type stars ($v_e \sin i \lesssim 50 \text{ km s}^{-1}$, $7000 \text{ K} \lesssim T_{\text{eff}} \lesssim 10000 \text{ K}$, many showing Am peculiarities to different degrees), based on high-dispersion and high-S/N spectral data secured at BOAO (Korea) and OAO (Japan). We found a significant trend that $A(\text{Na})$ tightly scales with $A(\text{Fe})$ irrespective of T_{eff} , which means that Na becomes enriched similarly to Fe in accordance with the degree of Am peculiarity. Regarding lithium, $A(\text{Li})$ mostly ranges between ~ 3 and ~ 3.5 (i.e., almost the same as or slightly less than the solar system abundance of 3.3) with a weak decreasing tendency with a lowering of T_{eff} at $T_{\text{eff}} \lesssim 8000 \text{ K}$, though several stars exceptionally show distinctly larger depletion. The abundances of potassium also revealed an apparent T_{eff} -dependence in the sense that $A(\text{K})$ in late-A stars tends to be mildly subsolar (possibly with a weak anti-correlation with $A(\text{Fe})$) systematically decreasing from ~ 5.0 ($T_{\text{eff}} \sim 8500 \text{ K}$) to ~ 4.6 ($T_{\text{eff}} \sim 7500 \text{ K}$), while those for early-A stars remain near-solar around ~ 5.0 – 5.2 . These observational facts may serve as important constraints for any theory aiming to explain chemical anomalies of A-type stars.

Key words: physical processes: diffusion — stars: abundances
— stars: atmospheres — stars: chemically peculiar — stars: early-type

1. Introduction

While elemental abundances in the photosphere of A-type stars, which are of particular interest because of the chemical anomalies of various types, have been extensively studied by a number of investigators so far, those of the alkali elements (Li, Na, and K) are barely known even nowadays, despite of their importance in stellar spectroscopy.

This is presumably due to the fact that these elements (with one valence electron weakly bound) are characterized by fairly low ionization potential (~ 4 – 5 eV) and most of them are ionized in the atmospheric condition of early-type stars, leaving only a tiny fraction as neutral. Since detecting spectral lines of the dominant ionized species is almost hopeless (because of the closed-shell configuration requiring vary large excitation energy), one is obliged to measure the very weak lines of neutral species (Li I, Na I, K I). Thus, the necessity of using sufficiently high-S/N spectra must have hampered past researchers from investigating the abundances of these elements.

Still, sodium has been comparatively well studied (e.g.,

Lane & Lester 1987; Varenne & Monier 1999; Gebran et al. 2008, 2010; Gebran & Monier 2008; Fossati et al. 2007, 2008) mainly by using subordinate lines (Na I 5682/5688 or 6154/6160) of moderate strengths (i.e., neither too strong nor too weak), which are less affected by the non-LTE effect. However, Na abundance determinations in A-type stars conducted so far are restricted to sharp-lined late-A stars ($T_{\text{eff}} \lesssim 8500 \text{ K}$) as well as F-type stars, and thus Na compositions of early-A through late-B stars ($T_{\text{eff}} \gtrsim 8500 \text{ K}$) remain essentially unexplored, except for our previous non-LTE investigations for the very bright stars of Sirius (Takeda & Takada-Hidai 1994) and Vega (Takeda 2008; hereinafter referred to as Paper I), and the recent LTE studies of Fossati et al. (2009) for two sharp-lined late-B stars (21 Peg and π Cet). Recently, Takeda et al. (2009; hereinafter referred to as Paper II) carried out an extensive non-LTE analysis of Na I resonance D lines at 5890/5896 Å for a large (122) sample of A-type stars ($7000 \text{ K} \lesssim T_{\text{eff}} \lesssim 10000 \text{ K}$) including rapid as well as slow rotators, with an aim to establish their Na abundance behaviors in general. Unfortunately, however, since the D lines are so strong and the resulting abundances are quite sensitive to the microturbulent velocity ξ , it turned out that ambiguities in the choice of ξ (which is likely to

* Based on data collected at Bohyunsan Optical Astronomy Observatory (KASI, Korea) and Okayama Astrophysical Observatory (NAOJ, Japan).

be depth-dependent and difficult to assign a value relevant for the high-forming strong D lines) prevented from precise sodium abundance determinations.

Almost the same situation holds for lithium: Determinations of Li abundances in A-type stars have been essentially restricted to late-A stars with $T_{\text{eff}} \lesssim 8500$ K (e.g., Burkhart & Coupry 1991a, 1991b, 1995, 2000; Burkhart et al. 2005; North et al. 2005), while early-A stars ($T_{\text{eff}} \gtrsim 8500$ K) remain practically untouched. Admittedly, this is a very difficult and challenging task, as the Li I 6708 line considerably weakens as T_{eff} becomes higher. The work of Paper I may be counted as an exceptional case, where the Li abundance of Vega could somehow be evaluated from the very weak Li I 6708 line ($EW \lesssim 1$ mÅ) based on a spectrum of ultra-high S/N ratio. Coupry and Burkhart (1992) reported the $EW(\text{Li I } 6708)$ of *o* Peg (a well-known very sharp-lined early-A star) to be 1.3 mÅ, which was used in Paper I (cf. Appendix A therein) to argue that the Li abundance of *o* Peg is almost consistent with the solar-system composition. However, as will be shown in this paper (cf. subsection 4.2), we consider that their measurement is an erroneous overestimation and Li is definitely underabundant in *o* Peg. This example well illustrates the enormous difficulty of Li abundance derivation in hot A-type stars.

Investigations of potassium abundances are even more lacking. As for late-A stars ($T_{\text{eff}} \lesssim 8500$ K), it is (to our knowledge) only the study of Fossati et al. (2007) that reported the K abundances of late-A and Am stars in the Praesepe cluster, though their neglect of the non-LTE effect (which may be significant for such a resonance line as K I 7699) prevented from obtaining reliable results (cf. subsection 4.4 therein). Meanwhile, almost nothing has been reported so far regarding the potassium abundances in early-A stars, except for Paper I where Vega’s K abundance could be successfully established.

It is thus evident that our current knowledge on the behaviors of alkali-element abundances in A-type stars is considerably insufficient. Given this situation, we decided to carry out a systematic spectroscopic study aiming at establishing the photospheric abundances of Na, Li, and K for an homogeneous sample of A-dwarfs ($7000 \text{ K} \lesssim T_{\text{eff}} \lesssim 10000 \text{ K}$) based on the spectral data of high quality. Since measurements of very weak lines are concerned in the present case (especially for early-A stars), we had to confine ourselves only to sharp-lined stars ($v_e \sin i \lesssim 50 \text{ km s}^{-1}$). This inevitably leads to the inclusion of a number of Am stars (metallic-lined A stars), which are characterized by deficiencies in comparatively light elements (C, N, O, Ca, Sc) as well as excesses of heavier elements (such as Fe-group or neutron-capture elements), since Am peculiarities are preferably observed in slow rotators (such as frequently seen in binaries). Accordingly, the purpose of this paper is to clarify and discuss the behaviors of Na, Li, and K abundances in slowly-rotating A-type stars based on the results of our analysis, while paying attention to the possible connection (if any exists) between these alkali elements and the

appearance/degree of Am anomalies.

2. Observational Data and Fundamental Parameters

2.1. Targets and Their Spectra

We selected 21 sharp-lined stars¹ satisfying $v_e \sin i \lesssim 50 \text{ km s}^{-1}$ from 122 A-type stars, studied in Paper II, where Na I 5890/5896 D lines were analyzed based on the spectra ($R \sim 45000$ and S/N ratios of a few hundreds) obtained by using BOES (Bohunsan Observatory Echelle Spectrograph) attached to the 1.8 m reflector at Bohunsan Optical Astronomy Observatory (BOAO). We call these 21 stars as “BOAO sample.” See section 2 of Paper II (and electronic table E therein) for more details about these observational data.

Besides, in order to augment the spectral data for early-A stars for which very high-quality is required to measure very weak lines of neutral alkalis, we also used the spectra of 7 bright sharp-lined stars (π Dra, α Lyr, α CMa, γ Gem, 15 Vul, 68 Tau, and *o* Peg), which were observed with the HIDES spectrograph (HIGH Dispersion Echelle Spectrograph; Izumiura 1999) attached to the 1.88 m reflector at Okayama Astrophysical Observatory (OAO). While the data of α Lyr were taken from the digital atlas (based on the observations carried out on 2006 May 1–4) published by Takeda, Kawanomoto, and Ohishi (2007) as in Paper I, those for the remaining 6 stars were secured by the observations on 2008 October 4 (15 Vul, 68 Tau, *o* Peg), October 7 (α CMa, γ Gem), and October 8 (π Dra). These 2008 OAO data, which cover the wavelength range of 4100–7800 Å with three mosaicked CCDs of 2K×4K pixels, have high spectral resolution ($R \sim 100000$) and very high S/N ratio (typically ~ 1000 , or even higher for the very bright α CMa and γ Gem). We call these 7 stars as “OAO sample.” Note that the following 4 stars are common to both of the BOAO and OAO samples: HD 172167= α Lyr, HD 48915= α CMa, HD 47105= γ Gem, and HD 27962=68 Tau. Accordingly, the actual (net) number of the targets is 24 (= 21 + 7 – 4). The list of these program stars is presented in table 1.

2.2. Atmospheric Parameters

Regarding the effective temperature (T_{eff}) and the surface gravity ($\log g$) of each program star, we simply adopted the values used in Paper II for 21 BOAO sample stars (including 4 OAO samples in common). As for the remaining 3 OAO stars, those for 15 Vul and *o* Peg were determined photometrically from Strömgen’s $b - y$, c_1 , and m_1 colors along with the β index by using Napiwotzki et al.’s (1993) calibration (as in Paper II; cf. subsection 3.1 therein), while the values derived by Adelman (1996) were adopted for π Dra (since color data were not available for this star). The final values of T_{eff} and $\log g$ are summarized in table 1. As can be seen in figure 1, where

¹ We discarded HD 112185 (ϵ UMa; magnetic Ap star) and HD 40932 (μ Ori; double-lined binary) because of their apparently unusual spectra, despite that these two stars have $v_e \sin i$ values less than 50 km s^{-1} .

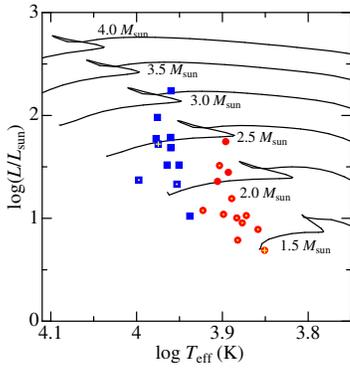


Fig. 1. Plots of the program stars on the theoretical HR diagram ($\log(L/L_{\odot})$ vs. $\log T_{\text{eff}}$), where the bolometric luminosity (L) was evaluated from the apparent visual magnitude with the help of the new Hipparcos parallax (van Leeuwen 2007) and Flower’s (1996) bolometric correction. Circles (red) — late A-type stars with $T_{\text{eff}} < 8500$ K, squares (blue) — early A-type stars with $T_{\text{eff}} > 8500$ K. Yellow dots (\cdot) and crosses ($+$) are overplotted for classical Am stars (i.e., those classified as “Am” in the spectral type given in the Bright Star Catalogue; cf. table 1) and Vega-like stars, respectively, in order to discriminate them from others. Theoretical evolutionary tracks corresponding to the solar metallicity computed by Girardi et al. (2000) for six different initial masses are also depicted for comparison.

the targets are plotted on the theoretical HR diagram, the mass values of the program stars range between $\sim 1.5 M_{\odot}$ and $\sim 3 M_{\odot}$. The model atmospheres for each of the stars were constructed by two-dimensionally interpolating Kurucz’s (1993) ATLAS9 model grid in terms of T_{eff} and $\log g$, where we exclusively applied the solar-metallicity models as in Takeda et al. (2008a) as well as Paper II.

2.3. Rotational Velocity, Microturbulence, and Abundances of O/Fe

Since we need to clarify the characteristics (e.g., parameters such as rotation or atmospheric turbulence, degree of abundance peculiarities) of our sample stars, a synthetic spectrum fitting analysis based on Takeda’s (1995) best-fit solution search algorithm was applied to the 6146–6163 Å region, in order to establish the projected rotational velocity ($v_e \sin i$), microturbulent velocity dispersion (ξ), and the abundances of iron and oxygen [$A(\text{Fe})$ and $A(\text{O})$; both are good indicators of Am anomaly; cf. Takeda and Sadakane (1997)] (along with that of Na as a by-product), similarly to what was done in Takeda et al. (2008a; cf. section IV therein) and Paper II (cf. subsection 3.2 therein). Actually, we varied seven free parameters ξ , $v_e \sin i$, $A(\text{O})$, $A(\text{Na})$, $A(\text{Si})$, $A(\text{Ca})$ and $A(\text{Fe})$ to accomplish the best fit, where the non-LTE effect was taken into account for O (as in Takeda et al. 2010) as well as for Na (as in Paper II). The adopted atomic parameters of important O, Na, and Fe lines relevant to this region are given in table 2. The instrumental broadening corresponding to the spectral resolving power was also taken into account, since sharp-lined stars are concerned here.

Since we could not find a reasonable ξ solution for the

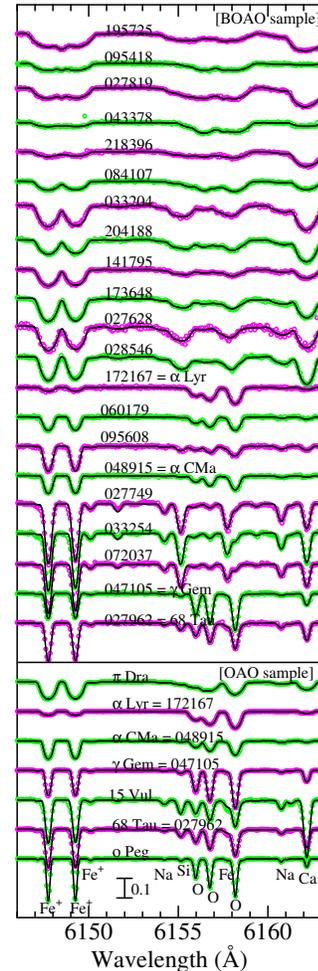


Fig. 2. Synthetic spectrum fitting at the 6146–6163 Å region while varying ξ , $v_e \sin i$, $A(\text{O})$, $A(\text{Na})$, $A(\text{Si})$, $A(\text{Ca})$ and $A(\text{Fe})$. The best-fit theoretical spectra are shown by solid lines, while the observed data are plotted by symbols. For each of the BOAO sample and OAO sample, the spectra are arranged (from top to bottom) in the descending order of $v_e \sin i$ as in table 1, and an offset of 0.1 is applied to each spectrum relative to the adjacent one.

following five BOAO cases (i.e., stabilized at an apparently unreasonable value, or any convergence could not be accomplished), we assumed an appropriate ξ value as fixed and repeated the iterations until convergence. $\xi = 2.5 \text{ km s}^{-1}$ (Adelman 1996; Monier 2005) for HD 95418, $\xi = 2.1 \text{ km s}^{-1}$ (Caliskan & Adelman 1997) for HD 43378, $\xi = 3.0 \text{ km s}^{-1}$ (Sadakane 2006) for HD 218396, $\xi = 3.9 \text{ km s}^{-1}$ (from the analytical formula derived by Takeda et al. 2008) for HD 204188, and $\xi = 2.53 \text{ km s}^{-1}$ (ξ solution from the OAO spectrum) for HD 48915. The finally adopted results of ξ , $v_e \sin i$, $A_{61}(\text{Fe})$, $A_{61}(\text{O})$, are presented in table 1 as well as in the electronic table E (where $A_{61}(\text{Na})$ is also given). How the theoretical and observed spectra match each other with the converged solutions of these parameters is shown in figure 2.

In figure 3, the resulting $A(\text{O})$ and $A(\text{Fe})$ values are

plotted against $v_e \sin i$ and T_{eff} , and their mutual correlation is also displayed.² We can see from these figures that the underabundance of O and the overabundance of Fe (both are the characteristics of Am peculiarities) are surely anti-correlated (figure 3c) and their weak $v_e \sin i$ -dependence is recognized (figures 3a,b) even in such a small range of $v_e \sin i$ (i.e., larger anomaly for slower rotators; cf. Takeda & Sadakane 1997). We also notice that two stars (HD 218396 and HD 172167=Vega) are apparently metal-deficient ($[\text{Fe}/\text{H}] \sim -0.5$), showing the abundance characteristics of Vega-like stars (cf. Sadakane 2006), which are presumably related to λ Boo stars (see, e.g., Paunzen 2004 and the references therein). It is interesting that these two appear to follow the O vs. Fe anti-correlation trend exhibited by Am stars, despite that interaction with interstellar clouds (cf. Kamp & Paunzen 2002; Paunzen et al. 2002) is becoming a promising mechanism for explaining the λ Boo phenomenon (instead of the diffusion process being considered as the standard theory for Am stars). Regarding the microturbulence, the ξ vs. T_{eff} relation depicted in figure 3e implies that the ξ values resulting from the 6146–6163 Å fitting are consistent with the analytical formula proposed by Takeda et al. (2008a) (which was invoked in Paper II).

2.4. Parameter Uncertainties and Their Impact on Abundances

In the next section (section 3) we will derive not only the abundances (of Na, Li, and K) but also the relevant abundance errors in response to the possible ambiguities in the adopted atmospheric parameters, where we estimate ± 300 K, ± 0.3 dex, and $\pm 30\%$ as the typical uncertainties in the absolute values of T_{eff} , $\log g$, and ξ , respectively. While the internal errors of our color-based T_{eff} and $\log g$ are ~ 200 K (2.5%) and ~ 0.1 dex according to Napiwotzki et al. (1993; cf. section 5 therein), we assumed somewhat larger ambiguities than these in view of the comparison with various published values (cf. section IV-c in Takeda et al. 2008a). The uncertainty in ξ was estimated from the dispersion³ in the ξ vs. T_{eff} relation (figure 3f).

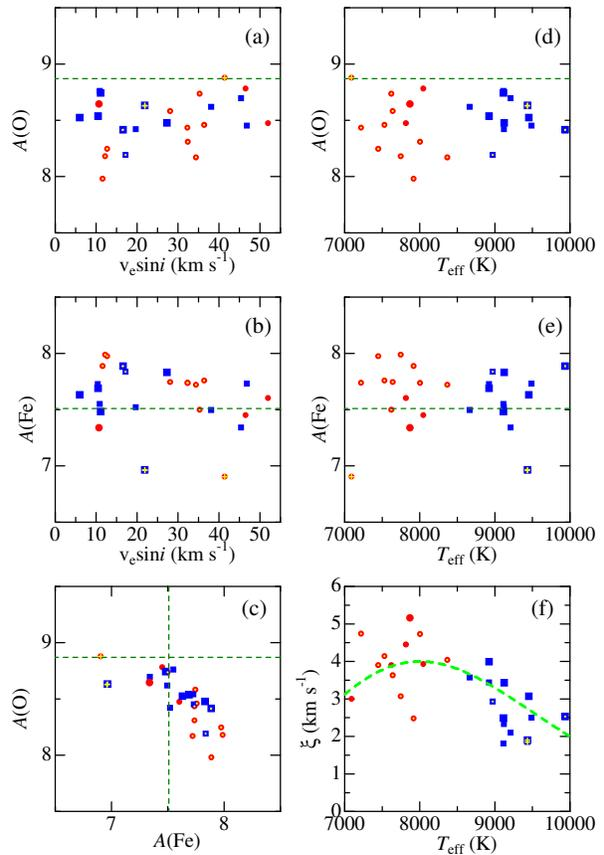


Fig. 3. Characteristics and mutual correlations of the abundances/parameters derived from the 6146–6163 Å region fitting, given in table 1. (a) $A(\text{O})$ (non-LTE oxygen abundance) vs. $v_e \sin i$ (projected rotational velocity), (b) $A(\text{Fe})$ (LTE iron abundance) vs. $v_e \sin i$, (c) $A(\text{O})$ vs. $A(\text{Fe})$, (d) $A(\text{O})$ vs. T_{eff} , (e) $A(\text{Fe})$ vs. T_{eff} , and (f) ξ (microturbulence) vs. T_{eff} . Circles (red) and squares (blue) correspond to stars with $T_{\text{eff}} < 8500$ K, and those with $T_{\text{eff}} > 8500$ K, respectively, where BOAO (smaller symbol) and OAO (larger symbol) results are discriminated by the symbol size. As in figure 1, (yellow) dots and crosses are overplotted for classical Am stars and Vega-like stars, respectively. The reference solar abundances are indicated by dashed lines in panels (a)–(e). In panel (f), the analytical approximation derived in Takeda et al. (2008a), $\xi = 4.0 \exp\{-[\log(T_{\text{eff}}/8000)/A]^2\}$ km s $^{-1}$ (where $A \equiv [\log(10000/8000)]/\sqrt{\ln 2}$), is also depicted by the dashed curve for comparison.

² The reference standard abundances indicated in figures 3, 5, 8, 10, and 11 in this paper are the solar photospheric abundances (solar-system meteoritic abundance only for Li) taken from Grevesse and Noels (1993; for Li, O, Fe) and Anders and Grevesse (1989; for Na, K).

³ This amount of dispersion ($\sim 30\%$) is regarded as a typical ambiguity in ξ , which can also be recognized by comparing various ξ values published so far (see, e.g., figure 1 in Coupry & Burkhart 1992; figure 2 in Gebran & Monier 2007). Yet, apart from this intrinsic dispersion, our ξ values tend to be somewhat larger than the previously reported results (usually based on EW values of Fe lines of various strengths). For example, our figure 3f suggests that the maximum ξ attained at mid-A type is ~ 4 – 5 km s $^{-1}$, while it is ~ 3 km s $^{-1}$ in figure 2 of Coupry and Burkhart (1992); also, our ξ results are systematically higher by ~ 1 km s $^{-1}$ with those of Landstreet et al. (2009), where 5 stars (68 Tau, γ Gem, α CMa, 15 Vul, and o Peg) are in common with our sample. We suspect that this may be due to a depth-dependence of ξ decreasing with height (cf. section 5 in Paper II). That is, our ξ -determination (based on 6146–6163 Å fitting) tends to reflect the physical condition in deeper layers (larger ξ) because of being mainly controlled by the deep-forming O I 6155–

Since resonance lines of alkali elements with low-ionization potentials are concerned in the present case, it is comparatively easy to understand (at least qualitatively) how the abundance is affected by changing each parameter. That is, since almost all atoms are in the ground state of the first-ionized (closed-shell) stage, and only a small fraction of them remain neutral, the number population of the ground level of the neutral atoms (n_1 , which is proportional to the line opacity l) is expressed as $n_1 \propto \epsilon \theta^{3/2} n_e 10^{\chi_I \theta}$ according to Saha's equation (ϵ is the abundance, $\theta \equiv 5040/T$, χ_I is the ionization potential ($\sim 4\text{--}5$ eV), and n_e is the electron density). Then, the dependence of the line-opacity (l) upon $\theta_{\text{eff}} (\equiv 5040/T_{\text{eff}})$ and g may be written as $l \propto \epsilon \theta_{\text{eff}}^{3/2} g^\alpha 10^{\chi_I \theta_{\text{eff}}}$ where we put $\theta \sim \theta_{\text{eff}}$ and used the approximation $n_e \propto g^\alpha$ ($\alpha \sim 1/3\text{--}2/3$ depending on T_{eff} ; see, e.g., Gray 2005). Consequently, the abundance (ϵ) resulting from a given equivalent width is strongly dependent upon θ_{eff} as $\epsilon \propto \theta_{\text{eff}}^{-3/2} 10^{-\chi_I \theta_{\text{eff}}}$ because of the exponential factor (i.e., ϵ increases as T_{eff} becomes higher). The $\log g$ -dependence is somewhat more complicated because the effect of the continuum opacity (κ) has to be taken into consideration. For late A-type stars of comparatively lower T_{eff} ($\sim 7000\text{--}8000$ K), H γ -opacity is still important and κ has almost the same g -dependence as l ; thus the abundances turn out rather independent on g because of the cancellation in the l/κ ratio determining the line strength (cf. Takeda et al. 2002). Meanwhile, for early A stars of higher T_{eff} where Paschen continuum opacity of neutral hydrogen is dominant, g -dependence in l directly reflects the line strength and the abundance scales as $\epsilon \propto g^{-\alpha}$ (i.e., ϵ decreases as $\log g$ becomes higher). Finally, regarding the effect of ξ (ϵ tends to decrease with an increase in ξ), the abundance results are practically inert to any change in ξ , since weak lines in the linear part of the curve of growth are concerned in most of the present cases (though only the Na abundances derived from Na I 5688 line for late A stars with $T_{\text{eff}} \lesssim 8000$ K exceptionally show some appreciable ξ -dependence; cf. figure 5f). We will show in section 3 that these expected trends can be actually confirmed by actual calculations (cf. figures 5, 8, and 10).

3. Abundance Determinations

3.1. $A(\text{Na})$ from Na I 5682/5688 fitting

The abundances of Na ($A_{61}(\text{Na})$) were already obtained from the fitting analysis in the 6146–6163 Å region (including Na I 6154/6160 lines) as described in subsection 2.3, which are given in electronic table E. However, while the Na I 6154/6160 lines are quite suitable for Na abundance determination for late-A stars, they become considerably weak as T_{eff} becomes higher and the accuracy of $A_{61}(\text{Na})$ may be comparatively low at early-A stars, especially for the non-metal-rich case (actually, $A_{61}(\text{Na})$ of HD 172167=Vega in the BOAO sample could not be

determined; cf. note 1 in electronic table E).

We therefore decided to determine the Na abundances from the spectra in the 5680–5690 Å region including the Na I 5682/5688 lines (stronger than Na I 6154/6160 while not too strong to be seriously sensitive to ξ). As done for the 6146–6163 Å region, we applied the fitting procedure to the 5680–5690 Å portion of the spectrum, where the telluric lines had been removed by dividing by the spectrum of a rapid rotator (cf. Paper I, Paper II). We varied five abundance parameters of $A(\text{Na})$, $A(\text{Si})$, $A(\text{Sc})$, $A(\text{Fe})$ and $A(\text{Ni})$ to obtain the best fit, while taking into account the non-LTE effect for Na as in Paper II (cf. table 2 for the atomic parameters of Na I 5682/5688). How the theoretical and observed spectra match each other with the converged solutions of these parameters is shown in figure 4. The resulting sodium abundances, $A_{56}(\text{Na})$, are given in table 1. Besides, as analysis-related quantities, the equivalent widths (EW) inversely computed from the abundance, the corresponding non-LTE corrections (Δ), and the abundance variations (δ) in response to each of the perturbations in T_{eff} (± 300 K), $\log g$ (± 0.3 dex), and ξ ($\pm 30\%$), which were computed for the Na I 5688 line following the procedure described in Paper II (cf. subsections 4.3 and 4.4 therein), are plotted against T_{eff} in figure 5. The (EW , Δ , δ) results for both Na I 5682 and 5688 lines are also presented along with $A_{56}(\text{Na})$ in electronic table E.

The comparison of the two sodium abundances [$A_{61}(\text{Na})$ and $A_{56}(\text{Na})$] derived from different regions/lines is displayed in figure 6. We can see from this figure that the agreement is good especially for late-A stars (red circles). The star showing the largest departure (~ 0.4 dex) is Vega (OAO sample) where $A_{61}(\text{Na}) = 5.63$ and $A_{56}(\text{Na}) = 6.05$ were derived, which is due to the low accuracy of A_{61} caused by the extreme weakness of Na I 6154/6160 lines in this star (cf. figure 3 in Paper I).⁴ We hereafter adopt $A_{56}(\text{Na})$ as the representative sodium abundances which we will discuss in subsection 4.1.

3.2. $A(\text{Li})$ from Li I 6708 equivalent width

We derived the abundance of Li from the EW of the merged Li I doublet feature at ~ 6708.8 Å. Since very

⁴ This result for Vega ($A_{61}(\text{Na}) = 5.63$) based on the 6146–6163 Å region fitting is considerably different from the EW -based value of 6.26 ($= 6.36 - 0.10$; cf. table 1 in Paper I), despite that both are based essentially on the same lines and the same non-LTE corrections. We understand that the reason for this marked discrepancy is the erroneous underestimation of the 6146–6163 Å fitting-based result (5.63) in this study. Namely, while the synthetic fitting method applied to a spectrum extending over some range (e.g., ~ 10 Å) is generally useful for simultaneous determinations of several elements at a time, it is not suitable for such a case where *extremely* weak line features are under question. That is, even a slight fluctuation of the continuum level can be a crucial source of error, because an appropriate adjustment of the local continuum is impossible in such a global spectrum synthesis. Accordingly, when one has to derive an abundance from an extremely weak line, the classical line-by-line EW analysis (adopted in Paper I) should be preferable. This is actually the reason why we adopted the classical EW -based abundance determination for Li and K, because the lines of these elements become very weak in early-A stars.

⁸ triplet lines of high excitation, while the conventional method using EW s of high-forming strong lines may yield comparatively lower ξ .

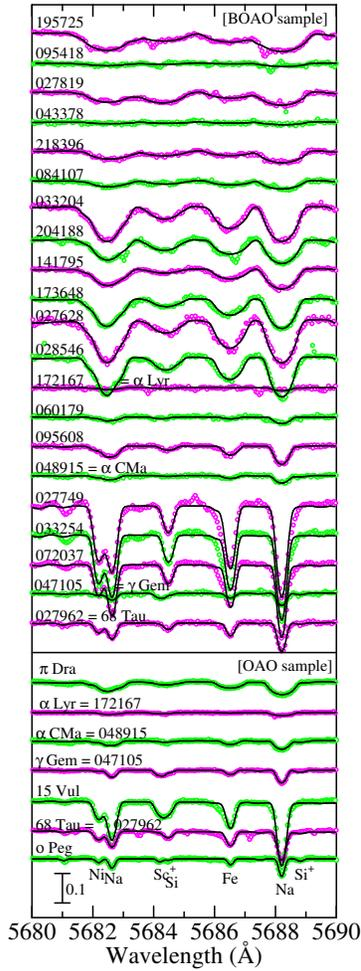


Fig. 4. Synthetic spectrum fitting at the 5680–5690 Å region while varying $v_e \sin i$, $A(\text{Na})$, $A(\text{Si})$, $A(\text{Sc})$, $A(\text{Fe})$, and $A(\text{Ni})$. The best-fit theoretical spectra are shown by solid lines, while the observed data are plotted by symbols. Otherwise, the same as in figure 2.

weak lines are generally concerned, EW measurements were carried out by the Gaussian fitting while comparing the spectrum on the computer screen with the theoretical spectrum synthesized with the known $v_e \sin i$ as well as appropriately varied $A(\text{Li})$, by which we tried to minimize the possibility of erroneous measurement.

In case we could not detect any suitable feature at the expected position, we gave up determination of EW . Actually, we were unable to specify $EW(6708)$ for about $\sim 50\%$ of the targets (13 out of the 21 BOAO sample and 2 out of the 7 OAO sample). In such cases, only the upper limit values were derived by the formula

$$EW^{\text{UL}} \equiv k \times \text{FWHM}/(S/N) \quad (1)$$

(cf. Takeda & Kawanomoto 2005). Here, FWHM was estimated from the root-sum-square of (i) the rotational broadening $w_r (\simeq 2 \times 0.78 v_e \sin i \lambda/c)$ (cf. footnote 12 of Takeda et al. 2008b), (ii) the approximate separation of the doublet $d (\simeq 0.15 \text{Å})$, and (iii) the instrumental

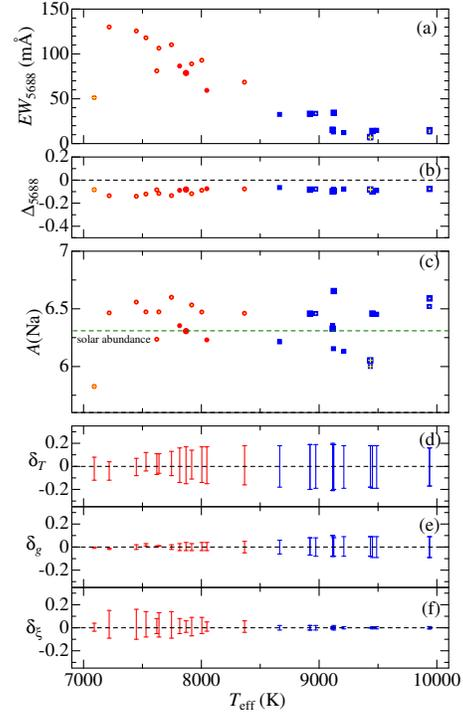


Fig. 5. Sodium abundances derived from the synthetic spectrum fitting in the 5680–5690 Å region, along with the abundance-related quantities specific to the Na I 5688.21 line, plotted against T_{eff} . (a) EW_{5688} (equivalent width), (b) Δ_{5688} (non-LTE correction), (c) $A(\text{Na})$ (non-LTE sodium abundance). (d) δ_{T+} and δ_{T-} (abundance variations in response to T_{eff} changes of +300 K and –300 K), (e) δ_{g+} and δ_{g-} (abundance variations in response to $\log g$ changes of +0.3 dex and –0.3 dex), and (f) $\delta_{\xi+}$ and $\delta_{\xi-}$ (abundance variations in response to perturbing the standard ξ value by $\pm 30\%$). See subsection 2.4 for the description on the parameter uncertainties. The signs of δ 's are $\delta_{T+} > 0$, $\delta_{T-} < 0$, $\delta_{g+} < 0$, $\delta_{g-} > 0$, $\delta_{\xi+} < 0$, and $\delta_{\xi-} > 0$. The meanings of the filled symbols are the same as in figure 3.

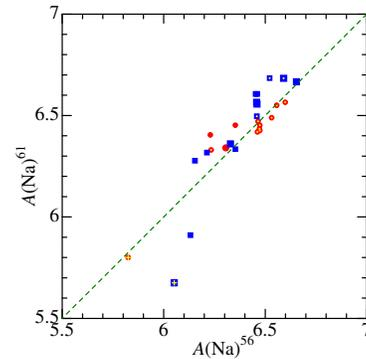


Fig. 6. Comparison the (non-LTE) sodium abundances derived from the 6146–6163 Å fitting [$A(\text{Na})^{61}$] and those from the 5680–5690 Å fitting [$A(\text{Na})^{56}$; finally adopted in this study]. The same meanings of the symbols as in figure 3.

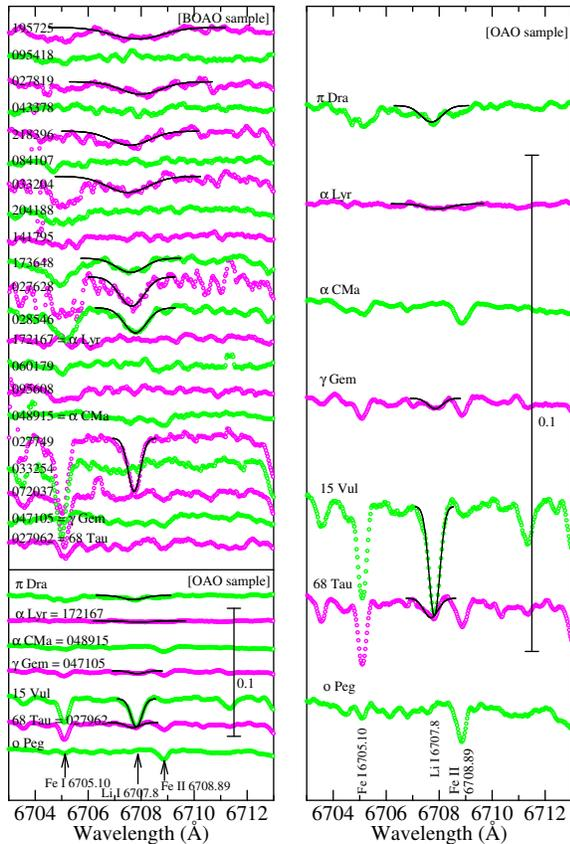


Fig. 7. [Left panel] Observed spectra (symbols) in the 6703–6713 Å region comprising the Li I 6708 line. For each of the BOAO and OAO samples, the spectra are arranged in the descending order of $v_e \sin i$ and shifted by 0.02 relative to the adjacent one. The Gaussian profiles fitted for EW measurements (when measurable) are depicted by solid lines. [Right panel] Spectra of seven OAO sample stars as given in the lower region of the left panel, but with the magnified vertical scale for the purpose of recognizing very weak features.

broadening $w_i (\simeq R\lambda/c)$ (R : spectrum resolving power), as $\text{FWHM} \equiv (w_r^2 + d^2 + w_i^2)^{1/2}$, and k was assumed to be 2 according to our experience. The actual measurements of $EW(6708)$ were carried out on the “smoothed” spectrum after applying the 9-pixel boxcar function to the original spectrum in order to reduce the effect of noise.⁵ Figure 7 displays how the Gaussian fitting for measuring EW was done in the relevant Li I 6708 region of the spectra.

Then, based on such evaluated EW (or EW^{UL}) and the model atmosphere along with the non-LTE departure coefficients (appropriately interpolated from the precom-

⁵ While how this smoothing process can improve the appearance of the spectrum is demonstrated in figure 6 of Paper I, the EW value (0.7 mÅ) of α Lyr at that time was actually measured in the “original” spectrum. In this study, however, the measurement was done on the “smoothed” spectrum, which is the reason for the appreciably larger value (1.2 mÅ) derived for this star in spite of the use of the same spectrum data of Takeda et al. (2007). This fact implies the difficulty in evaluating EW of extremely weak line feature, which is subject to considerable uncertainties.

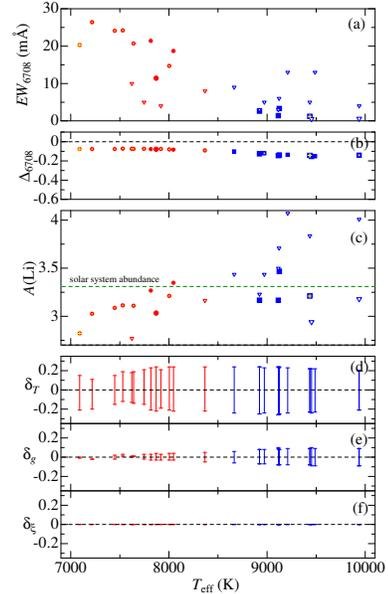


Fig. 8. Lithium abundances, along with the abundance-related quantities specific to the Li I 6708 line (comprising several components), plotted against T_{eff} . (a) EW_{6708} (equivalent width), (b) Δ_{6708} (non-LTE correction), (c) $A(\text{Li})$ (non-LTE lithium abundance), The meanings of panels (d), (e), and (f) are the same as in figure 5. See the caption of figure 3 for the differences in type and size of the filled symbols (circles and squares) as well as for the meanings of overplotted dots and crosses. The open (inverse) triangles indicate the upper limit values for the non-detection cases. In panel (f), the extents of δ_ξ are so small (because of the extreme weakness of the line) that they are hardly recognizable to eyes.

puted ones on a model grid; cf. Takeda and Kawanamoto 2005 for more details of the non-LTE calculations), $A(\text{Li})$ (non-LTE abundance) or its upper limit was determined for each star (see table 2 for the adopted atomic parameters) as given in table 1. Besides, in the similar manner as in subsection 3.1, we also computed the corresponding non-LTE corrections (Δ), and the abundance variations (δ) in response to perturbations of the atmospheric parameters. These [EW , Δ , $A(\text{Li})$, δ] results are plotted against T_{eff} in figure 8, which are also presented in electronic table E.

3.3. $A(K)$ from K I 7699 equivalent width

Regarding the abundance of K, we exclusively invoked the K I line at 7698.97 Å, since the alternative line of the doublet at 7664.91 Å tends to be severely influenced by strong telluric lines. Its EW was measured on the spectrum (in which telluric lines in the neighborhood had already been removed by dividing by that of a rapid rotator as in Paper I) in the same way as the case of the Li I 6708 line (cf. subsection 3.2). If the line failed to be detected (4 stars among the 21 BOAO sample), we estimated the upper limit (EW^{UL}) following equation (1), where $\text{FWHM} \equiv (w_r^2 + w_i^2)^{1/2}$ in this case. Figure 9 displays how these measurements were done in the relevant

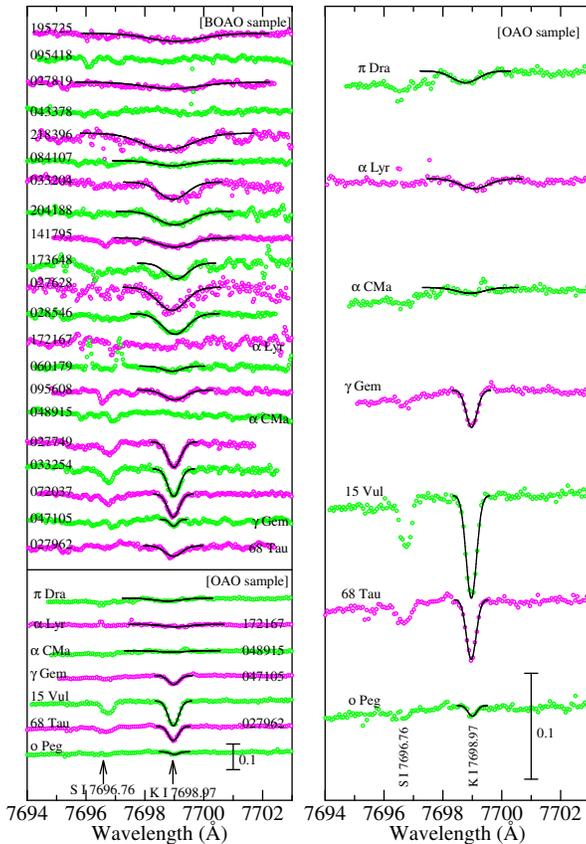


Fig. 9. Observed spectra (symbols) in the 7694–7703 Å region comprising the K I 7699 line. For each of the BOAO and OAO samples, the spectra are arranged in the descending order of $v_e \sin i$ and shifted by 0.1 relative to the adjacent one. Otherwise, the same as in figure 7.

K I 7699 region of the spectra.

Based on such evaluated EW along with the non-LTE departure coefficients (appropriately interpolated from the precomputed ones on a model grid; cf. Takeda et al. 1996 for more details of the non-LTE calculations), the non-LTE K abundance ($A(K)$) or its upper limit was determined for each star (with the atomic parameter of the line in table 2), as given in table 1. These results of EW and $A(K)$, along with the corresponding non-LTE corrections (Δ) and the abundance variations (δ) in response to perturbations of the atmospheric parameters, are plotted against T_{eff} in figure 10, and are also presented in electronic table E.

4. Discussion

We are now ready to answer the questions which motivated this study (cf. section 1): “How do the abundances of Na, Li, and K behave in sharp-lined A-type stars? How are they related with the Am peculiarities frequently seen in slow rotators of this T_{eff} range?” In figure 11 are plotted the resulting $[A(\text{Na}), A(\text{Li}), \text{and } A(\text{K})]$ against $A(\text{Fe})$ and $v_e \sin i$ (determined in subsection 2.3), both of which

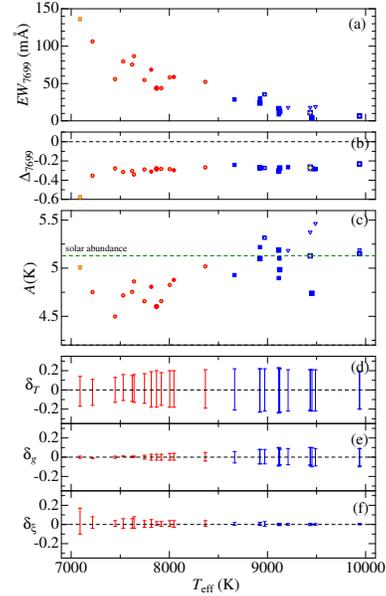


Fig. 10. Potassium abundances, along with the abundance-related quantities specific to the K I 7698.97 line, plotted against T_{eff} . (a) EW_{7699} (equivalent width), (b) Δ_{7699} (non-LTE correction), (c) $A(K)$ (non-LTE potassium abundance). The meanings of panels (d), (e), and (f), as well as the discriminations of the symbols are the same as in figure 8.

are the key quantities closely connected with the Am phenomenon. Based on this figure as well as figures 5c, 8c, and 10c (showing the T_{eff} -dependence), the abundance characteristics of these elements are discussed in the following subsections, where we also compare the observed trend with the theoretical prediction from the atomic diffusion theory by Richer, Michaud, and Turcotte (2000) as well as Talon, Richard, and Michaud (2006).

4.1. Sodium

Regarding Na, we notice in figure 11a a significant trend of remarkably tight correlation between $A(\text{Na})$ and $A(\text{Fe})$. Actually, a slight $v_e \sin i$ -dependence in $A(\text{Na})$ (similar to that seen for $A(\text{Fe})$ in figure 3b) is observed in figure 11a'. Since $A(\text{Fe})$ is known to be one of the Am indicators in the sense that larger overabundance of Fe is accompanied by stronger Am stars, this observational fact means that Na behaves in accordance with Fe (i.e., the excess of Na is a measure of Am anomaly just like that of Fe).

While Na abundances of Am(+Fm) and normal A(+F) stars (though mostly restricted to those with $T_{\text{eff}} \lesssim 8500$ K) in the field as well as in open clusters have been reported by several recent studies based on Na I 5683/5688 or 6154/6161 lines being less sensitive to non-LTE effects (e.g., Lane & Lester 1987; Varenne & Monier 1999; Gebran et al. 2008, 2010; Gebran & Monier 2008; Fossati et al. 2007, 2008), nobody seems to have explicitly mentioned this trend. However, an inspection of the results of these papers suggests tendencies of (i) moderately supersolar $[\text{Na}/\text{H}]$ and (ii) $[\text{Na}/\text{H}](\text{Am}) \gtrsim [\text{Na}/\text{H}](\text{normal A})$. Therefore, the existence of this positive correlation

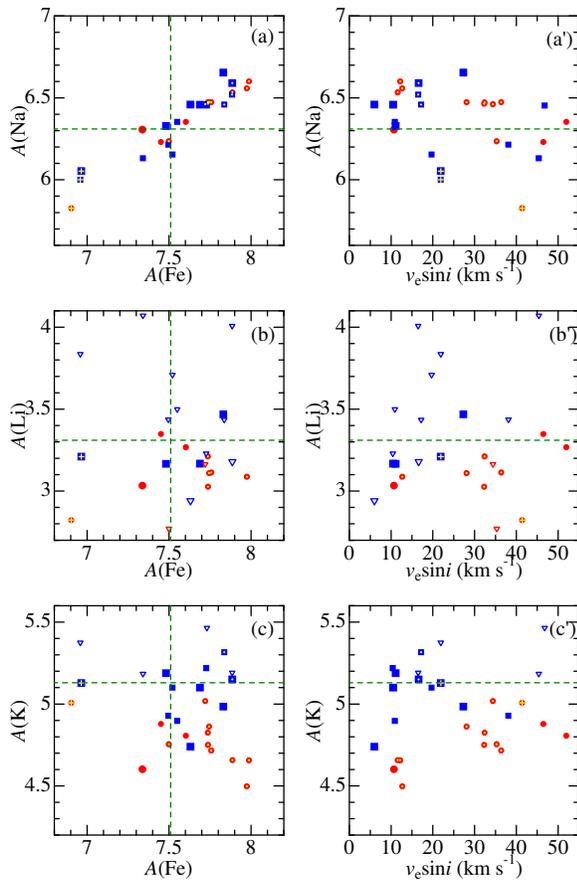


Fig. 11. The abundances of Na, Li, and K plotted against the Fe abundance (left panels; a, b, c) and the projected rotational velocity (right panels; a', b', c'). The reference solar abundances (solar system abundance for the case of Li) are indicated by dashed lines. The meanings of the filled symbols (as well as the overplotted dots and crosses) are the same as in figure 3, while the open (inverted) triangles indicate the upper limit values for the non-detection cases.

between $[\text{Na}/\text{H}]$ and $[\text{Fe}/\text{H}]$ appears almost certain.

From a theoretical point of view, however, such a conformance behavior between Na and Fe has never been predicted by any element segregation simulation designed for explaining Am peculiarities such as that of Richer et al. (2000) or Talon et al. (2006), which suggests that $[\text{Na}/\text{H}]$ remains almost solar or even slightly subsolar in spite of an appreciable overabundance of $[\text{Fe}/\text{H}]$ (cf. figure 14 of Richer et al. or figure 16 of Talon et al.). Therefore, the current diffusion theory (considered to be most promising for understanding the Am phenomena) is evidently imperfect at least in terms of Na, which remains to be improved. Here, the Na–Fe correlation revealed in this study would serve as an important observational constraint. Besides, it is interesting that the apparently metal-deficient stars with $A(\text{Fe}) \simeq 6.9\text{--}7.0$ (α Lyr and HD 218396=HR 8799) almost follow the same $A(\text{Na})\text{--}A(\text{Fe})$ relation defined by Am and normal stars with $7.3 \lesssim [\text{Fe}/\text{H}] \lesssim 8.0$. Since these two stars are known to be Vega-like stars (which may be related to so-called λ Boo stars; see, e.g., Kamp &

Paunzen 2002, Paunzen et al. 2002), there might be some connection between Am and λ Boo anomalies. (See also the last paragraph of subsection 2.3.)

4.2. Lithium

According to figures 11b and 11b', we do not see any clear $A(\text{Fe})\text{--}$ as well as $v_e \sin i\text{--}$ dependence in $A(\text{Li})$ which has values around or slightly lower than the solar-system abundance of ~ 3.3 . This may suggest that Am and normal A-type stars do not show any manifest difference in terms of their surface Li abundances.

We recognize, however, a tendency of T_{eff} -dependence for late A-type stars in the sense that $A(\text{Li})$ gradually decreases from ~ 3.3 ($T_{\text{eff}} \sim 8000$ K) to ~ 3.0 ($T_{\text{eff}} \sim 7000$ K) while such a systematic trend is not seen for early A-type stars ($T_{\text{eff}} \gtrsim 8500$ K) where $A(\text{Li})$ tends to be around the solar system abundance of ~ 3.3 (figure 8c). This T_{eff} -dependent tendency of $A(\text{Li})$ in late-A stars is also observed in figure 2 of North et al. (2005), and is more or less consistent with the theoretical prediction by Richer et al. (2000; cf. figure 14 therein).

It should be noted, however, that several stars apparently deviate from this general trend and show considerable Li-deficiencies (i.e., only the upper limit was derived since the Li line could not be detected). Here, especially important are the following 4 stars: HD 204188 (7622 K, < 2.77), HD 141795 (8367 K, < 3.16), o Peg (9453 K, < 2.94), and α CMa (9938 K, < 3.18). What makes such an exceptional depletion of Li? All these are classified as Am stars (o Peg is also an Am star according to Adelman 1988, though the conventional type of A1 IV is given in table 1), though Am alone can not be the condition to trigger such a marked underabundance of Li, because there are a number of other Am stars that do show normal behavior of Li. Actually, most of the present sample of low $v_e \sin i$ stars more or less show some degree of chemical peculiarities. In this connection, Burkhardt and Coupry (1991a) stated (based on their study of late A-type stars) that “occurrence of Li-deficient stars is not exceptional without any clearcut division between normal and Am stars.” Yet, as far as early A-type stars are concerned, the fact that Li tends to remain almost unaffected in near-normal stars such as γ Gem (believed to have almost the solar abundances; e.g., Adelman & Philip 1996, Lehmann et al. 2002) and π Dra (which were previously considered as normal even though later found to have only weak Am anomaly; cf. Sadakane & Okyudo 1990) might suggest the existence of some connection between the conspicuous Li deficit of α CMa or o Peg and their Am phenomenon.

Here, we have to remark that the conclusion of Paper I (the photospheric Li abundance of o Peg almost coincides with that of the solar-system composition; cf. Appendix A therein), which was based on the $EW(\text{Li } 6708)$ value of 1.3 mÅ taken from table 1 of Coupry and Burkhardt (1992), was not correct. As can be seen from figure 7, the Li I 6708 line is not detectable even on the spectrum of S/N ~ 1000 ; and we derived the upper limit of its equivalent width as $EW(6708) \lesssim 0.5$ mÅ (cf. the electronic table E) following equation (1). We suspect, therefore, that

Coupry and Burkhart (1992) misidentified/mismeasured this line, since the quality of their spectrum with typical S/N of ~ 300 (cf. section 1 therein) is evidently insufficient for measuring such an extremely weak line. Our revised conclusion for *o* Peg is $A(\text{Li}) \lesssim 2.94$, which means that its photospheric Li abundance is at least by $\gtrsim 0.4$ dex deficient compared to the solar-system value.

4.3. Potassium

Regarding $A(\text{K})$, we can observe (from figure 10c) a trend in terms of T_{eff} just similar to the case of $A(\text{Li})$: $A(\text{K})$ of late A-type stars appears to systematically decrease from ~ 5.0 ($T_{\text{eff}} \sim 8500$ K) to ~ 4.6 ($T_{\text{eff}} \sim 7500$ K), while such a systematic trend is not seen for early A-type stars ($T_{\text{eff}} \gtrsim 8500$ K) where $A(\text{K})$ is almost solar around ~ 5.0 (an exception is *o* Peg which shows a clearly subsolar abundance of ~ 4.7). Meanwhile, it also appears that $A(\text{K})$'s of late A-type stars are weakly dependent upon $A(\text{Fe})$ as well as $v_e \sin i$ in the sense that K gets more deficient as the Am anomaly becomes stronger (cf. the red circles in figures 11c and 11c'). Accordingly, the deficiency of K (particularly seen in late-A stars of $T_{\text{eff}} \lesssim 8500$ K) may be controlled by two factors (T_{eff} and the degree of Am peculiarity).

Richer et al.'s (2000) simulation based on the theory of atomic diffusion (along with radiative acceleration) predicts a small overabundance of K at higher T_{eff} (~ 10000 K) region, whereas a marginal underabundance is expected at the lower T_{eff} side (~ 7000 K) (cf. figure 14 therein). Such a predicted trend of positive $dA(\text{K})/dT_{\text{eff}}$ gradient is in qualitative agreement with what we found from figure 10c.

As mentioned in section 1, K-abundance determinations of A-type stars have so far been tried only by Fossati et al. (2007) in their LTE analysis of the K I 7699 line for late-A stars in the Praesepe cluster. According to their results for 5 stars, we see $\langle [K/H] \rangle_{\text{LTE}} \sim +0.2$ (± 0.3) (cf. figure 10 and table 3 therein). Considering that the typical (negative) non-LTE corrections amount to ~ 0.3 – 0.4 dex at the relevant T_{eff} range (cf. figure 10b), we may state that their results would turn out to be mildly subsolar when the non-LTE effect is taken into consideration, and become more consistent with our conclusion.

5. Conclusion

Motivated by the fact that our current understanding on the abundances of alkali elements in A-type stars is considerably insufficient, we conducted a comprehensive non-LTE analysis to establish the photospheric abundances of Na, Li, and K for 24 selected sharp-lined A-type stars ($v_e \sin i \lesssim 50$ km s $^{-1}$, 7000 K $\lesssim T_{\text{eff}} \lesssim 10000$ K), many of which are Am stars showing different degree of chemical peculiarity.

For this purpose, we primarily invoked the spectra of moderately high-dispersion ($R \sim 45000$) and high S/N ratio (typically a few hundreds) obtained with BOES at BOAO/Korea, though spectra of much higher quality ($R \sim 100000$ and S/N $\gtrsim 1000$) secured with HIDES

at OAO/Japan were additionally used for 7 apparently bright stars (mostly of early A-type).

We first carried out spectrum fitting analyses applied to the 6146–6163 Å region and derived ξ , $v_e \sin i$, $A(\text{O})$, and $A(\text{Fe})$, from which the degree of Am characteristics for each star could be confirmed.

The abundances of sodium, which were determined by the spectrum fitting method applied to the region comprising Na I 5682/5688 lines, revealed a significant trend that $A(\text{Na})$ tightly scales with $A(\text{Fe})$, which means that Na becomes enriched similarly to Fe in accordance with the degree of Am phenomenon. This result should be regarded as important because it seriously contradicts the prediction from the atomic diffusion theory.

Regarding lithium, $A(\text{Li})$ derived from the weak Li I line at 6708 Å showed a tendency of T_{eff} -dependence for late A-type stars in the sense that $A(\text{Li})$ gradually decreases from ~ 3.3 ($T_{\text{eff}} \sim 8000$ K) to ~ 3.0 ($T_{\text{eff}} \sim 7000$ K), while $A(\text{Li})$ for early A-type stars ($T_{\text{eff}} \gtrsim 8500$ K) tends to be around the solar system abundance of ~ 3.3 . However, several stars apparently deviating from this general trend and showing marked underabundances do exist, though what triggers such a Li deficiency is not clear.

The abundances of potassium derived from the K I 7699 line revealed a tendency somewhat similar to the case of lithium: An apparent T_{eff} -dependence (and possibly with a weak anti-correlation with Am peculiarity) exists for late-A stars where $A(\text{K})$ tend to be mildly subsolar systematically decreasing from ~ 5.0 ($T_{\text{eff}} \sim 8500$ K) to ~ 4.6 ($T_{\text{eff}} \sim 7500$ K), whereas those for most early-A stars remain near-solar around ~ 5.0 – 5.2 .

When these observational facts are compared with the theoretical prediction of Richer et al. (2000) or Talon et al. (2006) based on their atomic diffusion calculations, a serious discrepancy is found for Na (almost no anomaly or slightly subsolar tendency is predicted, while an enrichment of Na just like Fe is suggested from our analysis), though the simulated results appear to qualitatively reproduce the general trends observed for Li and K. Further improvement and development on the theoretical side would be desirably awaited to explain the results concluded in this study, which may serve as important constraints for any theory aiming to account for the origin of chemical anomalies in Am stars.

This research has made use of the SIMBAD database, operated by CDS, Strasbourg, France. I. Han acknowledges the financial support for this study by KICOS through Korea–Ukraine joint research grant (grant 07-179). B.-C. Lee acknowledges the Astrophysical Research Center for the Structure and Evolution of the Cosmos (ARSEC, Sejong University) of the Korea Science and Engineering Foundation (KOSEF) through the Science Research Center (SRC) program.

References

- Adelman, S. J. 1996, MNRAS, 280, 130
- Adelman, S. J. 1988, MNRAS, 230, 671

- Adelman, S., & Philip, A. G. D. 1996, *MNRAS*, 282, 1181
- Anders, E., & Grevesse, N. 1989, *Geochim. Cosmochim. Acta*, 53, 197
- Burkhart, C., & Coupry, M. F. 1991a, *A&A*, 249, 205
- Burkhart, C., & Coupry, M. F. 1991b, *Mem. Soc. Astron. It.*, 62, 91
- Burkhart, C., & Coupry, M. F. 1995, *Mem. Soc. Astron. It.*, 66, 357
- Burkhart, C., & Coupry, M. F. 2000, *A&A*, 354, 216
- Burkhart, C., Coupry, M. F., Faraggiana, R., & Gerbaldi, M. 2005, *A&A*, 429, 1043
- Caliskan, H., & Adelman, S. J. 1997, *MNRAS*, 288, 501
- Coupry, M. F., & Burkhart, C. 1992, *A&AS*, 95, 41
- ESA 1997, *The Hipparcos and Tycho Catalogues*, ESA SP-1200, available from NASA-ADC or CDS in a machine-readable form (file name: hip_main.dat)
- Flower, P. J. 1996, *ApJ*, 469, 355
- Fossati, L., Bagnulo, S., Landstreet, J., Wade, G., Kochukhov, O., Monier, R., Weiss, W., & Gebran, M. 2008, *A&A*, 483, 891
- Fossati, L., Bagnulo, S., Monier, R., Khan, S. A., Kochukhov, O., Landstreet, J., Wade, G., & Weiss, W. 2007, *A&A*, 476, 911
- Fossati, L., Ryabchikova, T., Bagnulo, S., Alecian, E., Grunhut, J., Kochukhov, O., & Wade, G. 2009, *A&A*, 503, 945
- Gebran, M., & Monier, R. 2007, in *Convection in Astrophysics*, ed. F. Kupka, I. W. Roxburgh, & K. L. Chan, *Proc. IAU Symp. 239* (Cambridge: Cambridge University Press), 160
- Gebran, M., & Monier, R. 2008, *A&A*, 483, 567
- Gebran, M., Monier, R., & Richard, O. 2008, *A&A*, 479, 189
- Gebran, M., Vick, M., Monier, R., & Fossati, L. 2010, *A&A*, 523, 71
- Girardi, L., Bressan, A., Bertelli, G., & Chiosi, C. 2000, *A&AS*, 141, 371
- Gray, D. F. 2005, *The Observation and Analysis of Stellar Photospheres*, 3rd ed. (Cambridge: Cambridge University Press), ch.9
- Grevesse, N., & Noels, A. 1993, in *Origin and Evolution of the Elements*, ed. N. Prantzos, E. Vangioni-Flam, & M. Cassé (Cambridge: Cambridge University Press), 15
- Hoffleit, D. 1982, *The Bright Star Catalogue*, 4th ed. (New Haven, Connecticut: Yale University Observatory)
- Izumiura, H. 1999, in *Proc. 4th East Asian Meeting on Astronomy, Observational Astrophysics in Asia and its Future* ed. P. S. Chen (Kunming: Yunnan Observatory), 77
- Kamp, I., & Paunzen, E. 2002, *MNRAS*, 335, L45
- Kurucz, R. L. 1993, *Kurucz CD-ROM*, No. 13 (Harvard-Smithsonian Center for Astrophysics)
- Kurucz, R. L., & Bell, B. 1995, *Kurucz CD-ROM*, No. 23 (Harvard-Smithsonian Center for Astrophysics)
- Landstreet, J. D., Kupka, F., Ford, H. A., Officer, T., Sigut, T. A. A., Silaj, J., Strasser, S., & Townshend, A. 2009, *A&A*, 503, 973
- Lane, M. C., & Lester, J. B. 1987, *ApJS*, 65, 137
- Lehmann, H., Andrievsky, S. M., Egorova, I., Hildebrandt, G., Korotin, S. A., Panov, K. P., Scholz, G., & Schönberner, D. 2002, *A&A*, 383, 558
- Monier, R. 2005, *A&A*, 442, 563
- Napiwotzki, R., Schönberner, D., & Wenske, V. 1993, *A&A*, 268, 653
- North, P., Betrix, F., & Besson, C. 2005, in *Element Stratification in Stars, 40 Years of Atomic Diffusion*, eds. G. Alecian, O. Richard, and S. Vauclair, *EAS Publication Series*, Vol. 17, p.333 (EAS)
- Paunzen, E. 2004, in *The A-Star Puzzle*, *Proc. IAU Symp. 224*, eds. J. Zverko, J. Žižňovský, S.J. Adelman, W.W. Weiss (Cambridge: Cambridge University Press), p.443
- Paunzen, E., Iliev, I. Kh., Kamp, I., & Barzova, I. S. 2002, *MNRAS*, 336, 1030
- Richer, J., Michaud, G., & Turcotte, S. 2000, *ApJ*, 529, 338
- Sadakane, K. 2006, *PASJ*, 58, 1023
- Sadakane, K., & Okyudo, M. 1990, *PASJ*, 42, 317
- Smith, V. V., Lambert, D. L., & Nissen, P. E. 1998, *ApJ*, 506, 405
- Takeda, Y. 1995, *PASJ*, 47, 287
- Takeda, Y. 2008, *MNRAS*, 388, 913 (Paper I)
- Takeda, Y., Han, I., Kang, D.-I., Lee, B.-C., & Kim, K.-M. 2008a, *JKAS*, 41, 83
- Takeda, Y., Kambe, E., Sadakane, K., & Masuda, S. 2010, *PASJ*, 62, 1239
- Takeda, Y., Kang, D.-I., Han, I., Lee, B.-C., & Kim, K.-M. 2009, *PASJ*, 61, 1165 (Paper II)
- Takeda, Y., Kato, K., Watanabe, Y., & Sadakane, K. 1996, *PASJ*, 48, 511
- Takeda, Y., & Kawanomoto, S. 2005, *PASJ*, 57, 45
- Takeda, Y., Kawanomoto, S., & Ohishi, N. 2007, *PASJ*, 59, 245
- Takeda, Y., Ohkubo, M., & Sadakane, K. 2002, *PASJ*, 54, 451
- Takeda, Y., & Sadakane, K. 1997, *PASJ*, 49, 367
- Takeda, Y., Sato, B., & Murata, D. 2008b, *PASJ*, 60, 781
- Takeda, Y., & Takada-Hidai, M. 1994, *PASJ*, 46, 395
- Talon, S., Richard, O., & Michaud, G. 2006, *ApJ*, 645, 634
- van Leeuwen, F. 2007, *Hipparcos, the New Reduction of the Raw Data* (Berlin: Springer)
- Varenne, O., & Monier, R. 1999, *A&A*, 351, 247

Table 1. Basic data of the program stars and the results of the analysis.

HD#	HR#	Name	Sp.type	T_{eff}	$\log g$	ξ	$v_e \sin i$	A_{Fe}	A_{O}	A_{Li}	A_{Na}	A_{K}	Remark
[BOAO sample]													
195725	7850	θ Cep	A7III	7816	3.74	4.45	52.0	7.60	8.47	3.27	6.35	4.81	
95418	4295	β UMa	A1V	9489	3.85	\dagger 2.50	46.8	7.73	8.45	(<4.34)	6.45	(<5.47)	
27819	1380	δ^2 Tau	A7V	8047	3.95	3.93	46.5	7.45	8.78	3.35	6.23	4.88	H
43378	2238	2 Lyn	A2Vs	9210	4.09	\dagger 2.10	45.4	7.34	8.70	(<4.07)	6.13	(<5.18)	
218396	8799	...	A5V	7091	4.06	\dagger 3.00	41.4	6.90	8.88	2.82	5.83	5.01	Vega-like star
84107	3861	15 Leo	A2IV	8665	4.31	3.57	38.1	7.50	8.62	(<3.44)	6.21	4.93	
33204	1670	...	A5m	7530	4.06	4.14	36.4	7.76	8.46	3.11	6.47	4.72	H
204188	8210	...	A8m	7622	4.21	\dagger 3.90	35.3	7.50	8.74	(<2.77)	6.24	4.75	
141795	5892	ϵ Ser	A2Vm	8367	4.24	4.04	34.4	7.72	8.17	(<3.16)	6.46	5.02	
173648	7056	ζ^1 Lyr	A4m	8004	3.90	4.73	32.4	7.74	8.31	3.21	6.47	4.82	
27628	1368	60 Tau	A3m	7218	4.05	4.74	32.3	7.74	8.43	3.03	6.46	4.75	H
28546	1428	81 Tau	A5m	7640	4.17	3.63	28.1	7.74	8.58	3.11	6.47	4.86	H
172167	7001	α Lyr	A0Va	9435	3.99	1.85	21.9	6.96	8.63	(<3.84)	6.00	(<5.38)	Vega-like star
60179	2891	α Gem	A1V	9122	3.88	2.33	19.7	7.52	8.42	(<3.71)	6.15	5.10	
95608	4300	60 Leo	A1m	8972	4.20	2.93	17.2	7.84	8.19	(<3.43)	6.46	5.32	
48915	2491	α CMa	A1Vm	9938	4.31	\dagger 2.53	16.5	7.89	8.41	(<4.01)	6.52	(<5.19)	
27749	1376	63 Tau	A1m	7448	4.21	3.90	12.7	7.97	8.25	3.09	6.56	4.50	H
33254	1672	16 Ori	A2m	7747	4.14	3.07	12.2	7.99	8.18	(<2.53)	6.60	4.66	H
72037	3354	2 UMa	A2m	7918	4.16	2.48	11.6	7.89	7.98	(<2.55)	6.53	4.66	
47105	2421	γ Gem	A0IV	9115	3.49	1.81	10.9	7.55	8.76	(<3.50)	6.35	4.90	
27962	1389	68 Tau	A2IV	8923	3.94	3.44	10.4	7.73	8.54	(<3.23)	6.46	5.22	H
[OAO sample]													
182564	7371	π Dra	A2III	9125	3.80	3.43	27.3	7.83	8.48	3.47	6.65	4.98	
172167	7001	α Lyr	A0Va	9435	3.99	1.90	21.9	6.97	8.63	3.21	6.05	5.13	Vega-like star
48915	2491	α CMa	A1Vm	9938	4.31	2.53	16.6	7.89	8.42	(<3.18)	6.59	5.15	
47105	2421	γ Gem	A0IV	9115	3.49	2.49	11.1	7.48	8.74	3.17	6.33	5.19	
189849	7653	15 Vul	A4III	7870	3.62	5.16	10.7	7.34	8.65	3.03	6.31	4.60	
27962	1389	68 Tau	A2IV	8923	3.94	3.99	10.5	7.69	8.54	3.17	6.46	5.10	H
214994	8641	o Peg	A1IV	9453	3.64	3.07	6.0	7.63	8.52	(<2.94)	6.46	4.74	

Note.

In columns 1 through 6 are given the HD number, HR number, star name (with constellation), spectral type (taken from Hoffleit 1982), effective temperature (in K), and logarithmic surface gravity (in cm s^{-2}). Columns 7 through 10 show the results derived from 6146–6163 Å region fitting: the microturbulent velocity (in km s^{-1}), projected rotational velocity (in km s^{-1}), (LTE) abundance of Fe, and (non-LTE) abundance of O. The non-LTE abundances of Li, Na, and K finally resulting from this investigation are presented in columns 11–13. All abundance results are expressed in the usual normalization of $A(\text{H}) = 12.00$. In each of the BOAO and OAO samples, the objects are arranged in the descending order of $v_e \sin i$. In the remark in column 14, Hyades cluster stars are denoted with “H”.

\dagger Regarding these ξ values, literature values were adopted unlike the others, because the ξ -determination from the 6146–6163 Å region fitting did not work successfully. See subsection 2.3 for more details.

Table 2. Atomic data of important lines relevant to the analysis.

Desig.	Species	$\lambda(\text{\AA})$	χ_{low} (eV)	$\log gf$
Li 6708	Li I	6707.756	0.00	-0.43
	Li I	6707.768	0.00	-0.21
	Li I	6707.907	0.00	-0.93
	Li I	6707.908	0.00	-1.16
	Li I	6707.919	0.00	-0.71
	Li I	6707.920	0.00	-0.93
O 6156	O I	6155.961	10.74	-1.40
	O I	6155.971	10.74	-1.05
	O I	6155.989	10.74	-1.16
O 6157	O I	6156.737	10.74	-1.52
	O I	6156.755	10.74	-0.93
	O I	6156.778	10.74	-0.73
O 6158	O I	6158.149	10.74	-1.89
	O I	6158.172	10.74	-1.03
	O I	6158.187	10.74	-0.44
Na 5682	Na I	5682.633	2.10	-0.70
Na 5688	Na I	5688.20 [†]	2.10	-0.40 [†]
Na 6154	Na I	6154.226	2.10	-1.56
Na 6160	Na I	6160.747	2.10	-1.26
Si 5684	Si I	5684.484	4.95	-1.65
Si 5688	Si II	5688.817	14.19	+0.40
Si 6155	Si I	6155.134	5.62	-0.40
S 7696	S I	7696.758	7.87	-0.89
K 7699	K I	7698.974	0.00	-0.17
Ca 6162	Ca I	6162.173	1.90	+0.10
Sc 5684	Sc II	5684.202	1.51	-1.05
Fe 5686	Fe I	5686.524	4.55	-0.63
Fe 6147	Fe II	6147.741	3.89	-2.72
Fe 6149	Fe II	6149.258	3.89	-2.72
Fe 6150	Fe II	6150.098	11.45	-3.26
Fe 6157	Fe I	6157.725	4.08	-1.26
Fe 6705	Fe I	6705.101	4.61	-1.50
Fe 6708	Fe II	6708.885	10.91	-0.52
Ni 5682	Ni I	5682.198	4.11	-0.47

Note.

All data are were taken from Kurucz & Bell's (1995) compilation, except for those of Li I which were adopted from Smith et al. (1998) as in Takeda and Kawanomoto (2005).

[†]Since this line comprises two close components of stronger $\log gf = -0.450$ (at 5688.205 Å) and weaker $\log gf = -1.400$ (at 5688.194 Å), we adopted $\log gf = -0.40$ as the sum of these two. Regarding the Li I lines, we considered only the lines of ⁷Li, since we neglected ⁶Li in our analysis.